ESCUELA DE CONSTRUCCIÓN CIVIL
FACULTAD DE INGENIERÍA

Revista de la Construcción
Journal of Construction

Research Article

Investigation of wear performance of GFRP profiles under different environmental conditions

Ferhat Aydın[1], Şeymanur Arslan[2], Süleyman Nurullah Adahi Şahin[*3], Elif Toplu[4]

1 Sakarya University of Applied Sciences, Sakarya (Turkey); ferhata@subu.edu.tr
2 Bartın University, Bartın (Turkey); seymanurarslan@bartin.edu.tr
3 Sakarya University of Applied Sciences, Sakarya (Turkey); adahisahin@subu.edu.tr
4 Sakarya University of Applied Sciences, Sakarya (Turkey); eliftoplu@subu.edu.tr
*Correspondence: adahisahin@subu.edu.tr (S. N. Adahi Şahin)

Received: 11.07.23; **Accepted:** 16.10.24; **Published:** 12.12.24

Citation: Aydın, F., Arslan, S., Şahin, S., and Toplu, E. (2024). Investigation of wear performance of GFRP profiles under dif-ferent environmental conditions. Revista de la Construcción. Journal of Construction, 23(3), 652-673. https://doi.org/10.7764/RDLC.23.3.652

Graphical Abstract:

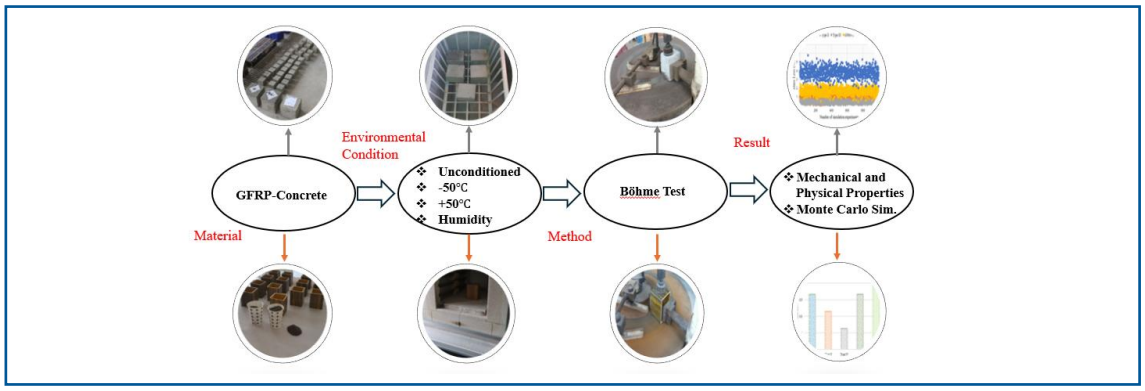

Highlights:

- The wear performance of GFRP box profiles under varying conditions was investigated.
- GFRP profiles showed increased wear at high temperatures, good performance in cold.
- Horizontal fiber direction in GFRP resulted in greater mass and volume loss.
- Concrete wear decreased with higher compressive strength and increased age.
- Monte Carlo Simulation was used to predict potential wear result ranges.

Abstract: Continuous exposure to external factors leads to loss of physical and mechanical properties in building materials due to wear effects. There is little information available on the wear performance of glass fiber reinforced polymer (GFRP) composite profiles, whose usage areas are increasing, under various conditions. In this study, the aim is to determine the wear performance of GFRP box profiles under different conditions. To evaluate the wear performance of GFRP profiles under

various conditions, their performance was compared with the wear performance of concrete under different strengths and conditions. The effects of fiber direction, temperature, and cold conditions on the wear performance of GFRP box profiles were investigated. The effects of compressive strength, age of concrete, humidity status, temperature, and cold conditions on the wear performance of concrete were experimentally determined and compared. The wear results of GFRP profiles tested in the Böhme wear test machine and the wear results of concrete in three strength classes were evaluated and compared under different conditions. In addition, the test numbers were increased using the Monte Carlo Simulation method to evaluate the possible result range. The wear losses of GFRP profiles increase with increasing temperature while they perform well under cold conditions. It was observed that GFRP box profiles in the horizontal fiber direction exhibited greater mass and volume loss. Concrete showed a decrease in mass loss as compressive strength increased. Similarly, the wear loss in concrete decreased as the age of the concrete increased, with the greatest mass and volume loss occurring in 3-day-old concrete.

Keywords: Wear, FRP profile, concrete, Böhme test, Monte Carlo simulation.

List of abbreviations:

FRP - fiber reinforced polymer
GFRP - glass fiber reinforced polymer
SD - standard deviation
V - vertical
H - horizontal.
T_g - glass transition temperature

1. Introduction

Structures are subject to various effects of nature over many years, and if not regularly maintained and repaired, they become unusable and lose their functions over time. Among the most commonly used building materials, concrete is prone to deformation due to external factors such as wind, water, as well as temperature, and acidic corrosion (Nochaiya, Suriwong, and Julphunthong 2022). These effects generate forces through friction and impact on the concrete surface, leading to surface wear. Surface wear is one of the most common forms of deterioration in concrete structures and has been a long-standing concern for durable concrete infrastructure elements (Mansouri et al. 2020; Wang et al. 2021). Concrete wear resistance is especially important for concrete surfaces exposed to moving objects and relative motion (Sharbaf, Najimi, and Ghafoori 2022). The wear resistance of concrete is related to the strength of the cement paste, aggregate properties, and the bond between the aggregate and cement (Kiliç et al. 2008; Y.-W. Liu, Cho, and Hsu 2012; Ramesh Kumar and Sharma 2014; Sadegzadeh, Page, and Kettle 1987). Many applications, such as improving surface treatments, improving coarse aggregate properties, and adding fibers or auxiliary components to concrete increase concrete wear resistance (Atiş 2002; He, Chen, and Cai 2019; Y. W. Liu 2007; Omoding, Cunningham, and Lane-Serff 2021a, 2021b; Silva et al. 2019; Zarrabi, Moghim, and Eftekhar 2021).

In recent years, different types of fiber-reinforced polymer (FRP) composites have been used as main building elements or strengthening materials in construction and infrastructure due to their lightness, high strength, high stiffness-to-weight ratio, and corrosion resistance properties (Aliasghar-Mamaghani and Khaloo 2018; Bakis et al. 2003; Choi et al. 2022; Christian and Billington 2011; Dweib et al. 2004; Jiang, Kolstein, and Bijlaard 2013; Keller 2001; Najafabadi et al. 2018; Teng et al. 2002, 2003; Shahrbijari et al. 2024). FRP composite materials have advantages in terms of strength, durability, life cycle cost, environmental impact performance, and exceptional mechanical properties (Hollaway 2010). Among the different fibers used in FRPs, glass fiber-reinforced polymers (GFRPs) are preferred because they are more economical and offer lower life cycle costs (Lee, Hong, and Park 2018; Nystrom et al. 2003; Aydin and Sarıbıyık 2010). FRP materials can be produced in various shapes, such as reinforcement bars, tendons, grids, and sheets, and are used for different purposes in the construction industry (CAN/CSA-S806-02 2009). GFRP profiles can be used as load-bearing structural elements, enabling the construction

of multi-story buildings, and GFRP box profiles have been used as the structural system in two-story buildings constructed in Türkiye (Aydin 2016). Additionally, a greenhouse has been built as part of a national project using GFRP profiles (Sarıbıyık et al. 2007). Numerous studies on FRP composites have shown that these materials can be used in place of traditional materials in some applications (Figure 1) (Singh et al. 2022; Aydin et al. 2018).

Figure 1. Structures built with GFRP profiles.

GFRP composite materials are as notable for their weaknesses as much as for their advantages. In particular, their performance being negatively affected under high temperatures, as well as their brittleness (Aydın F, et al 2024; Arslan Ş.and Aydın F. 2023) are significant factors that can limit the use of these materials. When exposed to high temperatures, GFRP materials can experience losses in mechanical properties, and their structural integrity may be compromised. For this reason, the thermal resistance of GFRP materials has become a significant research topic in many applications. GFRP bars were kept at 60 ℃ and -37 ℃ for 160 days and the losses in tensile strength were examined by Aydın and Arslan. The tensile strength of the bar exposed to 60 ℃ decreased by 5%, while the tensile strength of the reinforcement at -37 ℃ increased by 1% (Aydın F., andArslan Ş., 2021).

The compressive strength of GFRP profiles exposed to high temperatures was investigated by Khaneghahi et al. and observed that when the temperature exceeded 90 °C, which is near the glass transition temperature of the matrix, compressive strength was reduced by half (Khaneghahi, M. H.,et al 2020). Researches on the mechanical effects of high temperatures on FRP in the literature were reviewed by Bazli and Abolfazli and it was determined that, in general, exposure to high temperatures close to and above the resin glass transition temperature (T_g) has negative effects on the mechanical properties of FRP materials (Bazli, M., and Abolfazli, M. 2020). A study examining the compressive strength of GFRP bar at elevated temperatures found that GFRP bar retained most of its compressive strength when exposed to temperatures up to 60 ℃, but decreased significantly thereafter (AlAjarmeh, O Et al 2022).

In research where the tensile performance of GFRP composites at high and low temperatures was experimentally evaluated, it was reported that there was no significant effect on the tensile strength in the low temperature environment from room temperature to -20 °C, but a decrease in strength occurred as the temperature increased from 25 °C to 80 °C (Kumarasamy, S. et al 2018). The tensile performance of GFRP sheets at high temperatures was investigated by Jarrah et al. It was observed that, at temperatures between 25 and 150 °C, a decrease in tensile strength occurred due to softening of the epoxy adhesive at temperatures around T_g (Jarrah, M. et al 2018). Tensile properties of GFRP laminates were investigated after exposure to high temperatures. It was observed that profiles exposed to 70 °C for 20 minutes lost between 2% and 26% of their tensile strength (Ashrafi, H.,et al 2020). In studies where GFRP composites were exposed to high temperatures, it was determined that GFRP reinforcement retained 96.3% of its tensile strength at 100 °C (Özkal, F. M., et al 2018) and GFRP laminate retained 90% (Hawileh, R. A. et al 2015).

In a few studies investigating the wear performance of FRP materials, wear tests have been categorized and presented. Abrasive wear on FRP has been studied in two groups: two-body wear (Suresha et al. 2010; Suresha and Kumar 2009) and three-body wear (Agarwal, Patnaik, and Sharma 2014; Chand, Naik, and Neogi 2000; Suresha et al. 2008). There are also studies on erosion-induced wear (Harsha and Jha 2008; Tewari et al. 2003). While wear performance studies on GFRP materials (Chandru, B.G., and Shivashankar 2012; Das et al. 2019; Jumahat, Kasolang, and Bahari 2015; Lasri, Nouari, and Mansori 2011; Pihtili 2009; Srivastava 2006; Srivastava and Wahne 2007) have generally used different test methods and material types, few comparisons have been made with concrete using the same test setup.

Srivastava et al. (Srivastava and Wahne 2007) prepared randomly oriented short E-glass fiber reinforced epoxy resin composites filled with mica and tricalcium phosphate (TCP) particles using a hand lay-up method. The wear and friction behavior of these composites, sliding against AISI-1045 steel on a disk with a pin configuration, was evaluated using a TR-20LE wear and friction test machine. It was found that the filler particles significantly improved the mechanical properties and wear resistance of the E-glass fibers and increased the bonding strength between the filler particles and the epoxy resin. In another study, Lasri, Nouari, and Mansori (2011) performed progressive failure analyses to evaluate the wear resistance of FRP components used in aviation to analyze shear damage. When composite materials are processed at high speeds, the surface quality of the finished product can be improved by adjusting the processing parameters. Due to the complex nature of this process, the effect of cutting parameters on surface damage and, consequently, on the wear resistance of the processed component becomes significant. The analyses indicated that matrix cracking and interfacial sliding occurred first in the FRP material, followed by fiber wear. Damage progression in the matrix and interfacial regions was parallel to the fiber axis, suggesting that damage progression was strongly influenced by the fiber orientation of the FRP composite.

Pihtili (2009), investigated the effects of resin content on the wear of woven roving glass fiber-reinforced epoxy resin and glass fiber-reinforced polyester resin composite materials. Wear results were measured as mass loss. The study found that glass fiber-reinforced epoxy resin composites generally showed higher strength and lower wear than glass fiber-reinforced polyester resin composite materials. Another study investigating the wear properties of nano-silica-filled epoxy polymers and FRP composites (Jumahat, Kasolang, and Bahari 2015) used woven fiberglass as the reinforcement material. Fibers were mixed with epoxy resin modified with nano-silica in proportions of 5%, 13%, and 25% by weight. The results showed that increasing the amount of nano-silica reduced accumulated mass loss and significantly improved the wear resistance of the FRP composites.

In this study, glass fiber-reinforced polymer matrix composites produced by the hand lay-up method were tested for their mechanical properties and three-body dry sliding behavior by maintaining samples at 140 °C for six hours. The dry sliding test results indicated that the wear rate and specific wear rate of the GFRP composite sample were 0.11674 mm^3/m and 5.95×10^{-3} mm^3/Nm, respectively. Das et al. (2019) also examined the mechanical properties and three-body dry sliding behavior of glass fiber-reinforced polymer matrix composites produced by the hand lay-up method under similar conditions, obtaining the same wear rate and specific wear rate results.

In addition to previous studies, this research compared the wear performance of different types of concrete with GFRP profiles, considering the potential of GFRP box profiles as an alternative to traditional structural materials in some applications. Samples were tested at -50 °C and +50 °C to represent low and high air temperatures, respectively, for GFRP box profiles. The fiber orientation was varied to determine the effect on wear direction. For concrete, experiments were conducted with variables such as moisture, temperature, and age of the concrete. Mass and volume losses due to wear were evaluated using the Böhme wear test under various conditions. Furthermore, the relationship between simulation and experimental results was analyzed by replicating experimental outcomes using Monte Carlo simulations and conducting probability calculations.

2. Materials and methods

2.1. *Material*

The wear performances of GFRP box profiles and concrete specimens in 3 different strength classes were investigated under various conditions in experimental studies (Figure 2). The dimensions of all specimens were produced as 71 x 71 x 71 mm according to TS 2824 EN 1338 (2005) (TS2824 2005).

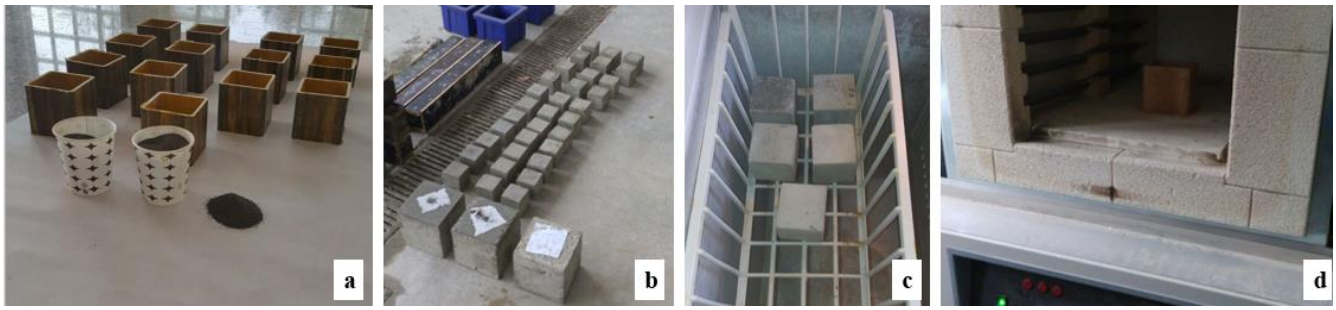

Figure 2. a) GFRP profiles, b) concrete samples, c) samples conditioned at low temperatures, d) samples conditioned at high temperatures.

The GFRP box profiles are hollow and produced using E-type glass fiber and polyester resin with a thickness of 4 mm. The properties of the fiber and resin are provided in Table 1. The fiber ratios of GFRP profiles were obtained experimentally. The masses of the profiles, kept in the oven until the matrix material evaporated, were measured after removal. The amount of matrix material was calculated by subtracting the mass after entering the oven from the mass before entering the oven. The remaining mass after oven treatment represents the mass of the fibers. The box profile consists of two layers, with felt fibers constituting a small amount on both the inside and outside of the profile. Longitudinal fibers are situated between these two felt fiber layers (Figure 3). As a result of the experiment, the felt fiber ratio of the GFRP profiles was determined to be 9%, while the longitudinal fiber ratio was found to be 42% (Table 2).

Samples measuring 4 x 250 x 2500 mm, obtained from the surface of GFRP box profiles, were subjected to tensile testing. Strain was measured using an extensometer, and the tensile strength was determined to be 374.44 MPa (Figures 4-5). The average compressive strength of the box profiles (71 x 71 x 71 mm) was determined to be 146 MPa.

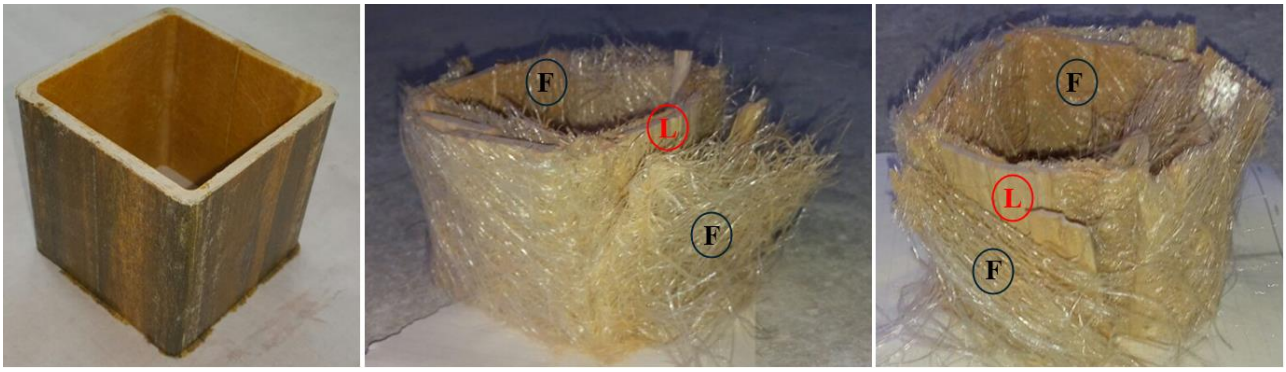

Figure 3. The felt (F) and longitudinal (L) glass fiber layers in the GFRP box profile.

Table 1. Glass fiber and resin properties.

Glass fiber: FWR6		Polyester resin: liquid CE 67 HV4	
Glass type	E	Tensile strength	Min 50 N/mm^2
Connector type	Silane	Flexural strength	Min 85 N/mm^2
Fiber diameter:	17	Hardness	Min. 45 barcol
Split tex	2400	Appearance	Clear
Roving tex	2400	Viscosity	1000±150 Cps
Roving tex (g/1000m)	300½410½600½900½1200½ 2400	Acid number	26.0-34.0 mgKOH/g
CE binding code	(06)	Additive	Min %65
Fiber diameter (m)	4 ½ 16 ½15 ½18 ½ 15 ½ 17	Gelation time (25 ℃)	4±1 minute
Resin compatibility	Polyester / vinyl ester / epoxy	Exothermic peak (25 ℃)	190 ±15 ℃
Humidity content	max. %0.15	Stability	3 months

Table 2. GFRP box profile properties.

Modulus of elasticity	Tensile strength	Poisson ratio	Unit weight	Specific gravity	Longitudinal fi-ber rate	Felt fiber ratio	Glass transition temperature
29000 N/mm^2	374,44 N/mm^2	0.33	1.75 g/cm^3	1.80	42 %	9 %	115 ℃

Figure 4. a) Tensile, and b) compressive test sample.

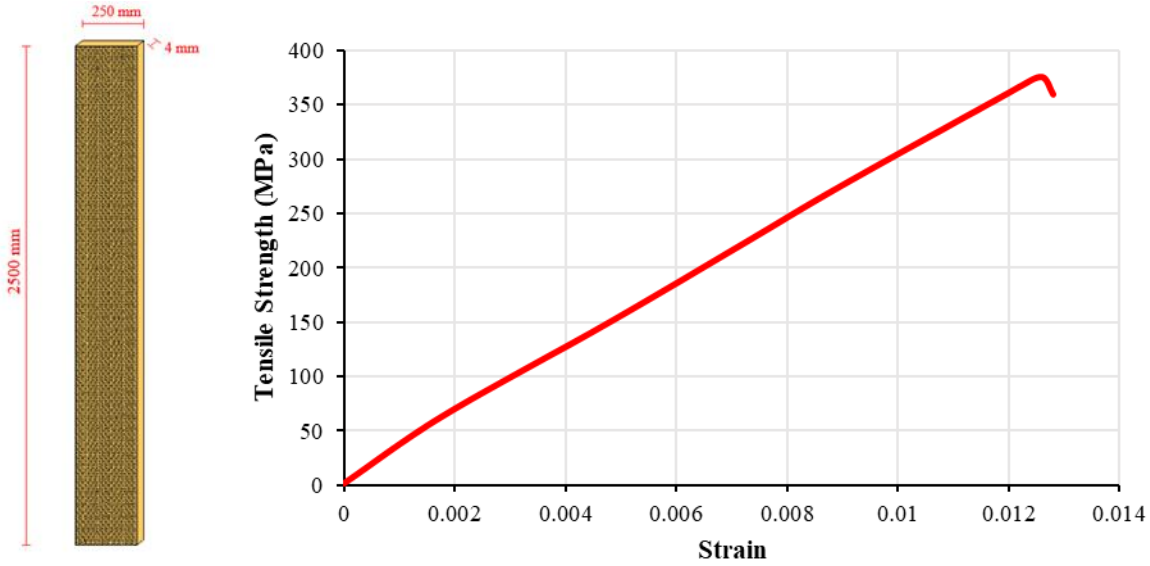

Figure 5. Tensile test sample and tensile stress – strain graph of GFRP.

Concrete specimens were produced in three strength classes to determine the effects of concrete strength on wear performance. Material mix ratios and 28-day average cube compressive strengths for each strength class are given in Table 3.

Table 3. Concrete material mixing ratios (kg/m^3).

Material (kg)	Type I	Type II	Type III
Cement	326	417	535.7
Water	225	225	225
Plasticizer additive	0	4.17	10.7
1 No. aggregate	1071	1025	965.2
0-4 No. aggregate	775.5	742.3	698.5
Total	2397.5	2413.5	2435.2
Compressive strength (MPa)	23.3	33.0	40.4

2.2. *Method*

The wear performances of GFRP box profiles under various environmental conditions and concrete specimens of different strengths were compared. Mass and volume losses were measured after wear tests, and comparisons were made between the specimens. Wear tests were conducted using the Böhme wear tester (Figure 6) for each specimen type, with five replicates for accuracy.

Figure 6. GFRP box profile and concrete wear tests.

Wear tests were conducted by planning scenarios to simulate various environmental conditions that GFRP materials and concrete might be exposed to. To assess the effect of fiber orientation on wear in GFRP profiles, experiments were conducted with samples positioned both vertically and parallel to the wear direction at room temperature (Figure 7). Additionally, wear tests were performed at +50 °C to represent high temperatures and -50 °C to simulate cold weather conditions.

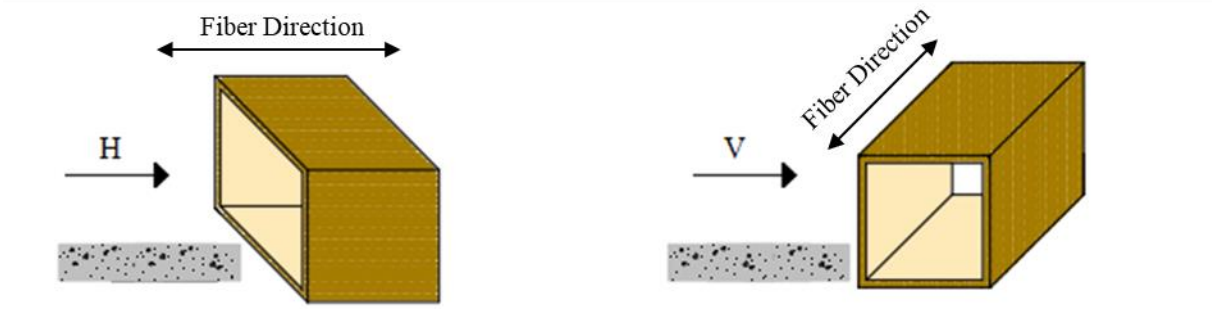

Figure 7. Experiment direction (H: horizontal, P: vertical).

To compare the wear performance of GFRP profiles, which are considered as new generation materials, with the most widely used construction material, concrete specimens with different strengths were tested for wear performance. For this purpose, the effects of 3, 7, and 28-day concrete ages, hot-cold environment conditions, and moisture content in the concrete were experimentally investigated, in addition to the strengths of concrete samples in three strength classes.

In addition to the experiments investigating the effects of concrete age, moist, hot, and frozen concrete samples were prepared after 28 days of curing, and the specified conditions were provided. In the investigation of the cold effect, the samples were kept at -50 °C and subjected to wear tests. In the temperature effect, the samples were kept in an oven and their temperatures were maintained during the wear test using a hot air gun. In the Böhme wear test, the samples were placed on a horizontal rotating abrasion disc with a diameter of 750 mm, rotating at a speed of 30 rpm and under a load of 294 N. In each test, 20 g of corundum abrasive powder was sprinkled on the rubbing strip, and the samples were subjected to a total of 22x16=352 revolutions of wear.

3. Experimental results

The results of the wear tests have been analyzed under two categories: mass loss and volume loss.

3.1. Mass loss

The average mass loss values obtained from the wear tests of GFRP box profiles parallel and vertical to the fiber axis are presented in Table 4 and their corresponding graphs are shown in Figure 8-9. In Figure 8 and 9, the error bars represent the standard deviation of the mass loss values. These standard deviations were calculated based on repeated tests under each condition to account for the variability in the measurements.

Table 4. Mass loss rates of GFRP box profiles.

Direction	Non-conditioned (%)	Standard deviation (%)	-50 ℃ (%)	Standard deviation (%)	+50 ℃ (%)	Standard deviation (%)
Vertical	1.63	0.37	1.00	0.35	2.88	0.18
Horizontal	3.80	0.55	1.19	0.42	5.05	0.22

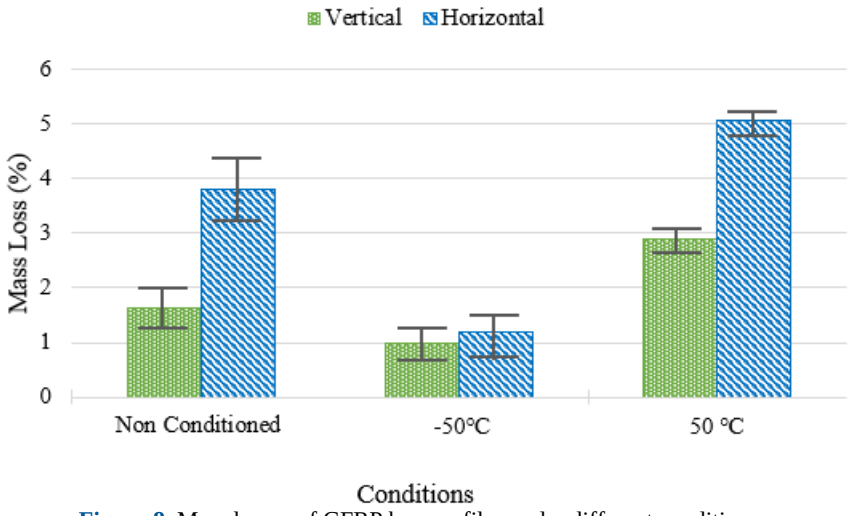

Figure 8. Mass losses of GFRP box profiles under different conditions.

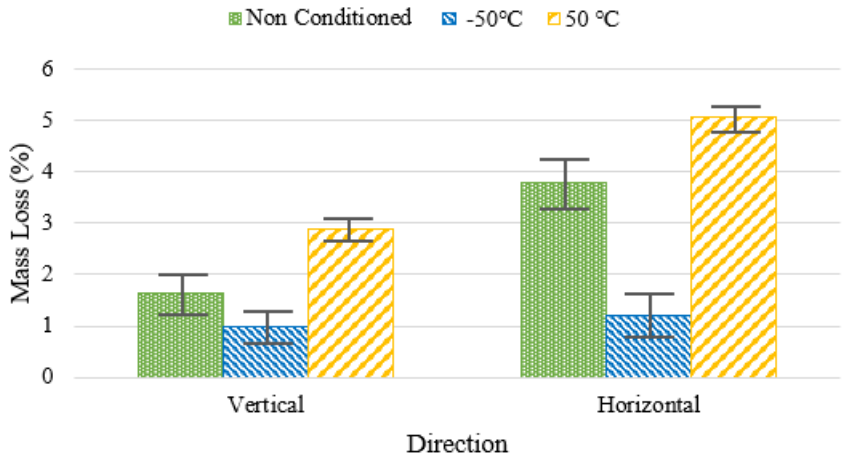

Figure 9. The effect of fiber orientation on wear resistance in GFRP box profiles.

It is well-known that the integrity of fibers and matrix decreases in FRP materials with increasing temperatures, leading to significant strength losses. In the wear tests, mass losses increased with temperature compared to room temperature. In the GFRP samples, those exposed to lower temperatures showed better wear performance, contrary to the effects observed at higher temperatures. In tests conducted vertical to the fibers without conditioning, mass losses at +50 °C increased by 77% compared to room temperature GFRP samples. Conversely, mass losses at -50 °C decreased by 39% compared to room temperature samples. In these tests, cold samples exhibited approximately three times less wear than hot samples. In parallel fiber tests, mass losses increased by 33% at +50 °C and decreased by 69% at -50 °C compared to reference GFRP samples at room temperature. Hot samples exhibited approximately 4.2 times more wear than cold samples.

In the wear tests, mass losses in GFRP profiles occurred primarily due to the wear of the resin matrix in the surface region. In tests vertical to the fibers, fewer mass losses were observed compared to tests parallel to the fibers. In these tests, the sandpaper dust rubbing against the GFRP material surface helped prevent the glass fibers from breaking away from the resin matrix. However, in parallel fiber tests, the wear axis and fibers were aligned in the same direction, reducing the protective effect of glass fibers against wear of the resin matrix. Furthermore, the differences in mass losses between vertical and horizontal fiber tests were limited in cold conditions. Mass losses in parallel fibers were 133% and 75% higher than in vertical

fibers for reference samples (room temperature) and hot samples (+50 °C), respectively, whereas this difference was only 19% for samples kept in cold conditions (-50 °C).

The wear performances of GFRP profiles, which are next-generation construction materials, were evaluated by comparing them with the wear data of traditional concrete samples under various conditions. Cubic concrete samples with different strength classes were subjected to wear tests under varying environmental conditions, and the resulting mass losses are presented in Table 5. The comparison of the graphs is shown in Figures 10 and 11.

Table 5. The mass loss rates of concrete types.

Concrete type	Concrete age (non-conditioned) (%)						Humidity (%)		-50 °C (%)		+50 °C (%)	
	3 days	SD	7 days	SD	28 days	SD	Loss (%)	SD (%)	Loss (%)	SD (%)	Loss (%)	SD (%)
I	1.61	0.14	1.30	0.15	1.04	0.38	1.11	0.18	1.1	0.26	1.01	0.10
II	1.13	0.17	0.89	0.31	0.69	0.10	0.81	0.06	0.69	0.22	0.78	0.03
III	0.91	0.31	0.81	0.24	0.36	0.16	0.54	0.09	0.38	0.13	0.60	0.07

SD: Standard deviation

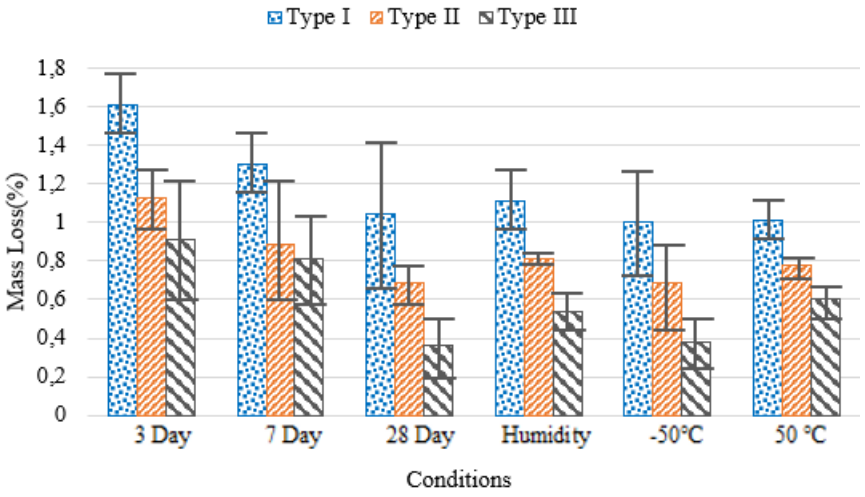

Figure 10. The effect of different conditions on the mass loss rate in concrete.

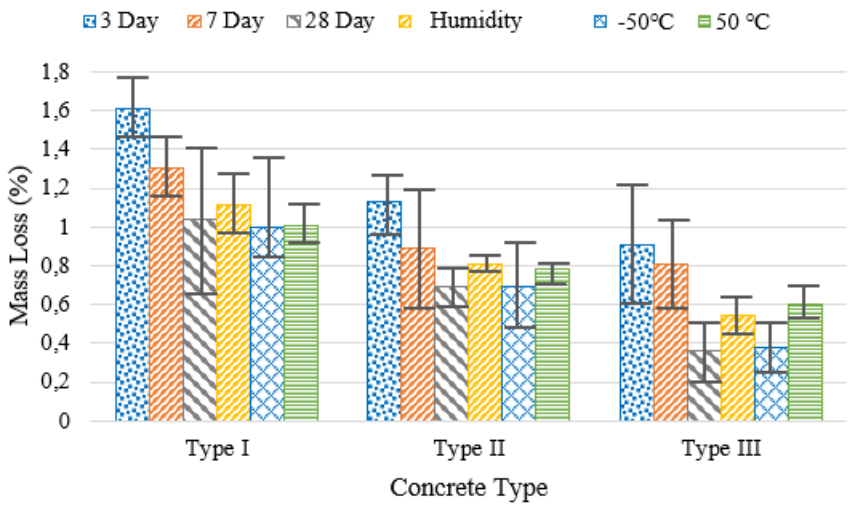

Figure 11. Mass loss rates in different types of concrete.

The average compressive strengths of concrete for Types I, II, and III are 23.3, 33.0, and 40.4 MPa, respectively. When examining the effects of compressive strength on the wear performance of concrete, it is observed that mass losses decrease as expected with increasing strength under all conditions. Mass losses decrease at every age of concrete as compressive strength increases. In 3-day-old concrete, mass losses of high-strength concrete (Type III) are 22% less than those of medium-strength concrete (Type II) and 77% less than those of low-strength concrete (Type I). The mass loss rates at 7 days are 10% and 60% less, respectively. At 28 days, these differences are 92% and 188%, respectively. In 28-day-old concrete, increasing strength results in mass losses of high-strength concrete being 22% less than those of medium-strength concrete (Type II) and 77% less than those of low-strength concrete (Type I).

When considering the effect of concrete age on wear, it was determined that the mass loss rates of 7-day and 3-day concrete samples for Type I concretes are 25% and 55% higher, respectively, than those of 28-day concrete samples. For Type II concretes, the mass loss rates of 7-day and 3-day concrete samples are 29% and 64% higher, respectively, than those of 28-day concrete samples. For Type III concretes, which have the highest strength, the mass loss rates of 7-day and 3-day concrete samples are 125% and 153% higher, respectively, than those of 28-day concrete samples. As concrete strength increases, the difference in mass loss rates due to concrete age also increases. The mass loss rates of 3-day concrete samples are 24%, 27%, and 12% higher than those of 7-day concrete samples for Types I, II, and III, respectively.

When examining the effects of sample temperatures on wear in concrete, it was found that in humid, hot samples (+50 °C), and frozen samples (-50 °C), compressive strength is highest in the strongest concretes, and the least amount of mass loss occurs, as expected. In the highest strength group (Type III), compared to normal condition concrete, moist concrete had a 50% higher mass loss rate, hot concrete had a 67% higher mass loss rate, and frozen samples had a 5% higher mass loss rate. For Type II concretes, the mass loss rates in moist, hot, and frozen samples were 17%, 13%, and 0%, respectively, compared to reference concrete. For low-strength Type I concretes, the mass loss rates in moist and hot samples were 7% and 3% higher, respectively, compared to reference concrete, while the mass loss rate in frozen samples decreased by 4%. As with GFRP profiles, cold samples showed the best performance against wear in concrete.

As concrete strength increases, surface hardness increases, and wear rates decrease. As moisture content increases, surface hardness decreases, and wear rates increase. Moist concrete becomes saturated with water, increasing its weight, though mass loss rates remain relatively low. It is well-known that the curing process of early-age concrete increases its strength. A 3-day-old concrete has completed 40% of its strength, a 7-day-old concrete has completed 65-70%, and a 28-day-old concrete has completed 95-99% of its strength. Therefore, an increase in wear resistance is expected to be observed in all three types of concrete as the curing time increases.

3.2. Volume loss

The volume losses observed in GFRP box profiles because of wear tests are given in Table 6 and comparison graphs are shown in Figure 12. It should be noted that the GFRP box profiles were hollow inside.

Table 6. Volume loss rates of GFRP box profiles according to the direction of wear.

Direction	Vertical (%)	Standard deviation (%)	Horizontal (%)	Standard deviation (%)
Non-conditioned	0.97	0.46	1.05	0.38

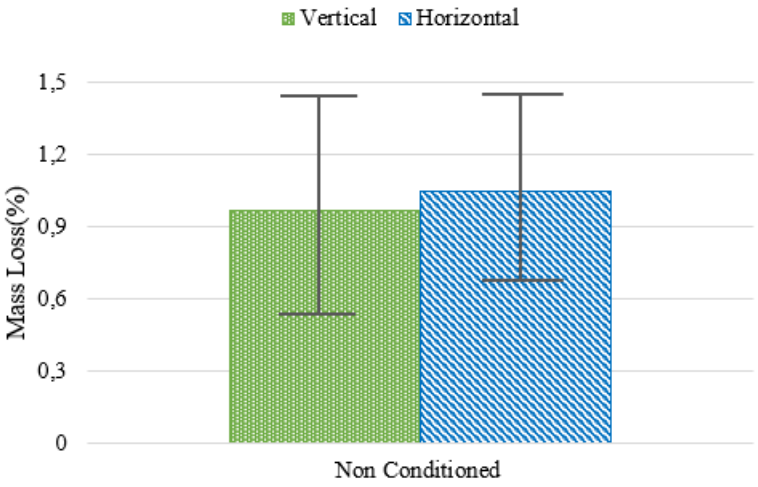

Figure 12. Comparison of volume loss rates in GFRP box profiles based on wear direction.

In the case of wear, similar volumetric losses were observed in GFRP box profiles for wear parallel to and vertical to the fiber axis. The volumetric loss rates due to wear parallel and vertical to the fiber axis were approximately 1%. It was observed that the volumetric loss rates in GFRP box profiles were lower than the mass loss rates. Volumetric losses in concrete samples due to wear are given in Table 7 and shown in Figures 13-14.

Table 7. Volume loss rates according to concrete types and environmental conditions.

Concrete type	Concrete age (non-conditioned) (%)						Humidity (%)		-50 °C (%)		+50 °C (%)	
	3 days	SD	7 days	SD	28 days	SD	Loss (%)	SD (%)	Loss (%)	SD (%)	Loss (%)	SD (%)
I	1.81	0.81	1.5	0.38	1.25	0.38	1.32	0.37	1.3	0.65	1.39	0.76
II	1.33	0.18	1.15	0.18	0.92	0.20	1	1.05	0.95	0.20	1.02	0.33
III	1.01	0.25	0.72	0.09	0.48	0.15	0.6	0.14	0.45	0.24	0.6	0.28

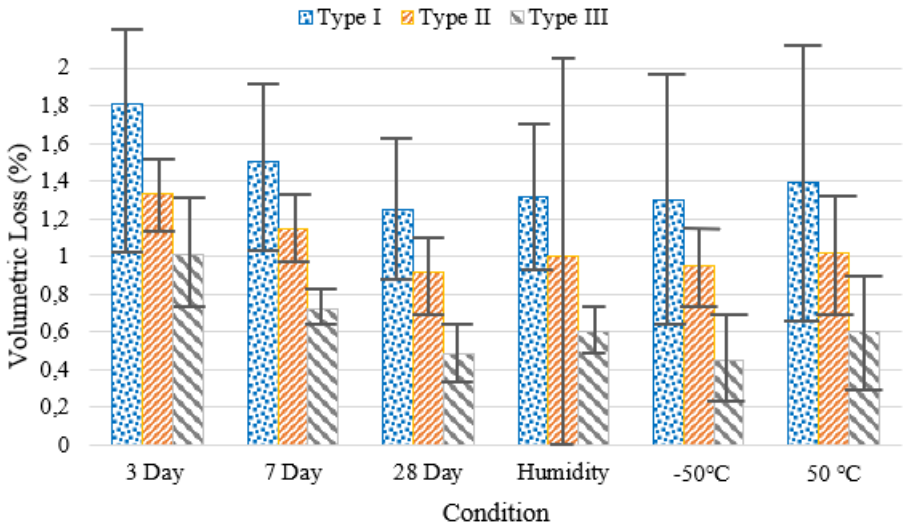

Figure 13. Volume loss rates under different environmental conditions.

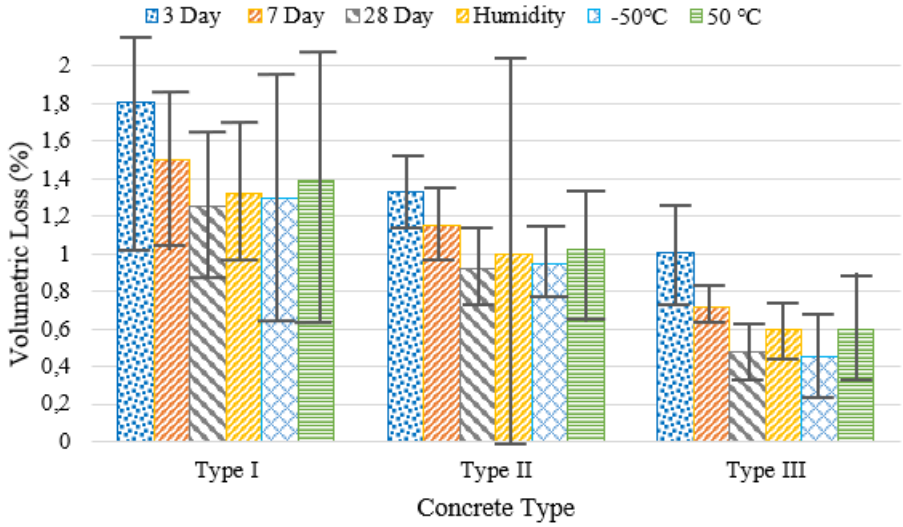

Figure 14. Volume loss rates of concrete types.

The volume losses in concrete samples are below 2% under all conditions. Volume losses decrease with the age and strength of the concrete. The volume losses in Type III and 3-day-old concrete samples are 32% and 79% less than in Type II concrete, respectively. This trend is observed to be 36% and 108% less in 7-day-old concrete samples. In 28-day-old concrete samples, the volume loss rates are 92% and 160% less with decreasing strength. The volume losses of high-strength Type III concrete samples at 28 days are 50% less than those in Type II concrete and 110% less than those in Type I concrete.

When evaluating the effect of concrete age on wear, it is determined that the volume loss rates of 7-day and 3-day-old concrete samples are 20% and 45% higher, respectively, than the volume loss rates of 28-day-old concrete samples in Type I concrete. In Type II concrete, the volume loss rates of 7-day and 3-day-old concrete samples are 25% and 45% higher, respectively, than those of 28-day-old concrete samples. In Type III concrete, these rates are 50% and 110% higher, respectively. The volume loss rates are 20%, 15%, and 40% higher for 3-day-old concrete samples compared to 7-day-old samples in Types I, II, and III, respectively.

When examining the effects of sample temperature and humidity on wear in concrete, it is determined that there is a 25% volume loss in humid and hot concrete compared to concrete under normal conditions, while there is 6% less volume loss in samples kept in cold conditions for Type III concrete. In Type II concrete, the volume loss rates of humid, hot, and cold samples are 9%, 11%, and 3% higher, respectively, compared to reference concrete. In Type I concrete, the volume loss rates of humid, hot, and cold samples are 6%, 11%, and 4% higher, respectively, compared to reference concrete.

4. Comparison of GFRP profiles and concrete wear

In this section of the study, the wear performance of GFRP profiles and concrete specimens under different environmental conditions was compared. It is known that as the concrete strength increases, the surface hardness also increases, and therefore, the wear performance also improves. The conditioned samples were compared, and the mass loss is presented in Figure 15 and the volumetric loss ratios in Figure 16 for all conditioned samples within the scope of this study.

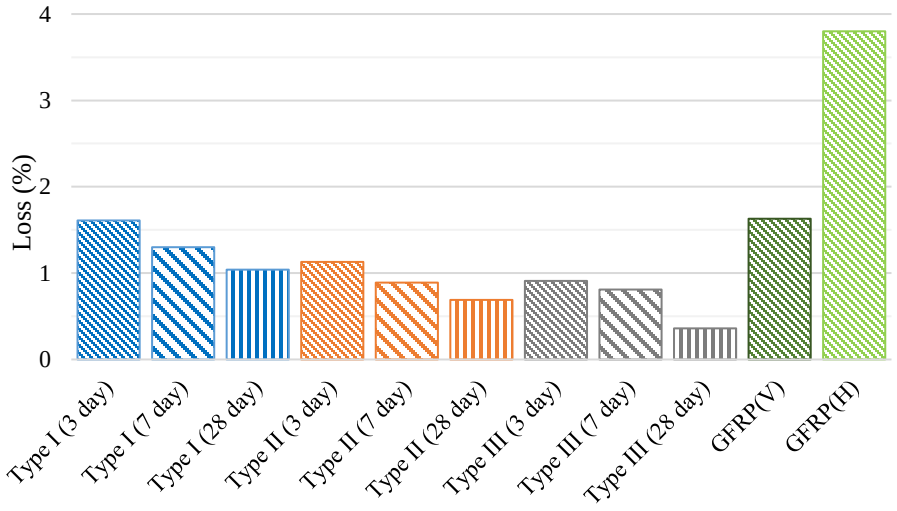

Figure 15. Mass losses of unconditioned samples.

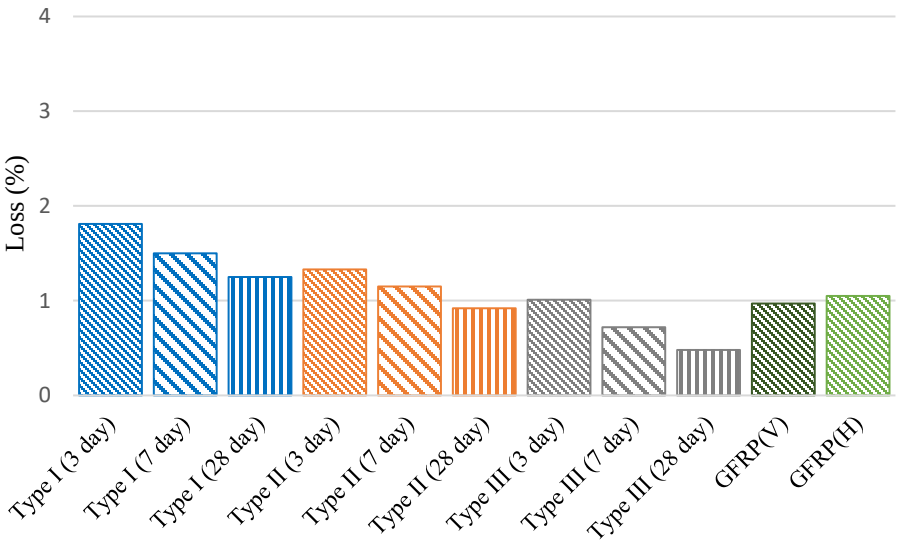

Figure 16. Volumetric losses of unconditioned samples.

The highest mass loss rate was observed in GFRP box profiles, while the volumetric loss rate was observed in the concrete specimens with incomplete strength. Due to the hollow structure of the GFRP box profiles, the total sample weight is low. In concrete specimens, the total sample weight is high, so the mass wear loss rates are relatively low in percentage terms. In GFRP profiles, the resin layer on the outermost layer is worn (Figure 17). Thus, the wear of the matrix material does not cause much variation in the volumetric wear rates, but it affects the mass wear loss rates more.

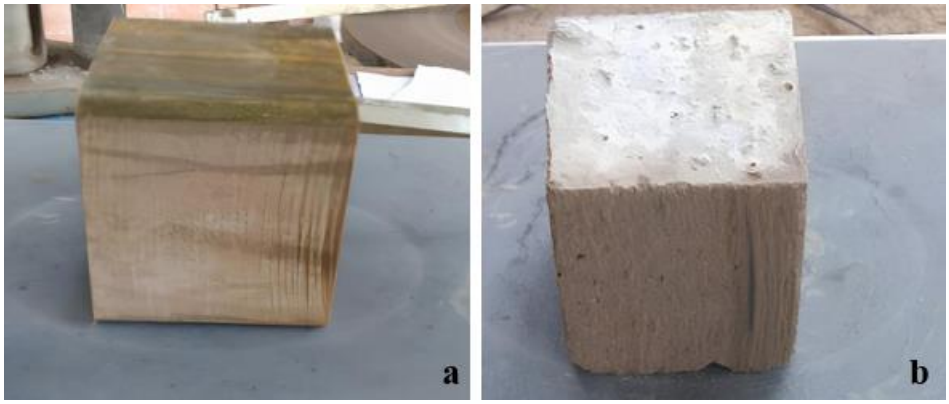

Figure 17. a) GFRP and concrete, b) specimen after wear test.

In the comparison of conditioned specimens in cold environments, the results of concrete specimens of three strength classes at 28 days and GFRP profiles under cold conditions were compared. The results showed that GFRP profiles exhibited the lowest wear resistance when wear occurred parallel to the fiber axis, while the best result was achieved by the Class III concrete specimens (Figure 18).

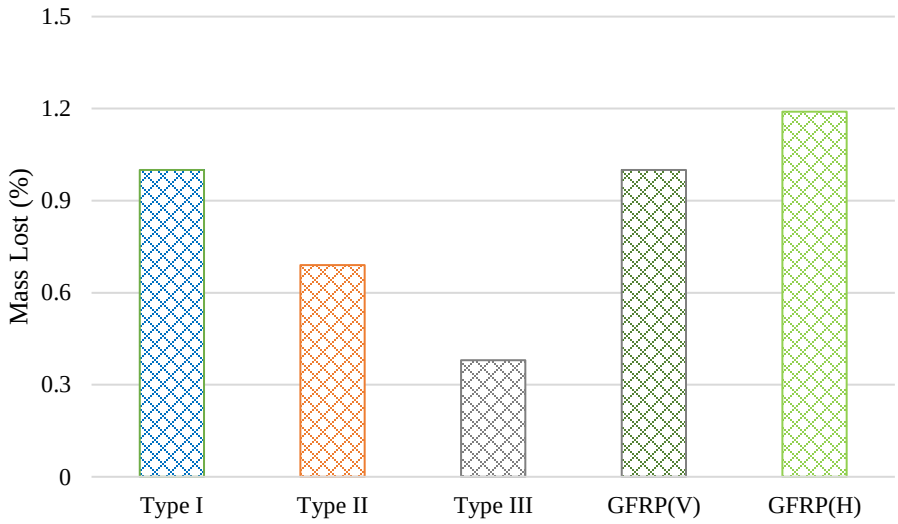

Figure 18. Mass losses of -50 ºC conditioned samples.

Since the matrix material of GFRP profiles is polymer, they have a low melting temperature. As the temperature increases, the binding matrix in the polymers begins to soften, and the glass transition temperature varies depending on the matrix material in the GFRP profiles. Generally, this value varies between 80-130 °C, and as it approaches this value, strength losses increase. The mass losses of GFRP samples conditioned at +50 °C are given in Figure 19. A 5% wear loss was observed parallel to the fibers and approximately 2.9% wear loss was observed vertical to the fibers in GFRP profiles, and it was determined that fibers reduce wear. Type I concrete, which is the lowest strength class, showed a 1% wear loss.

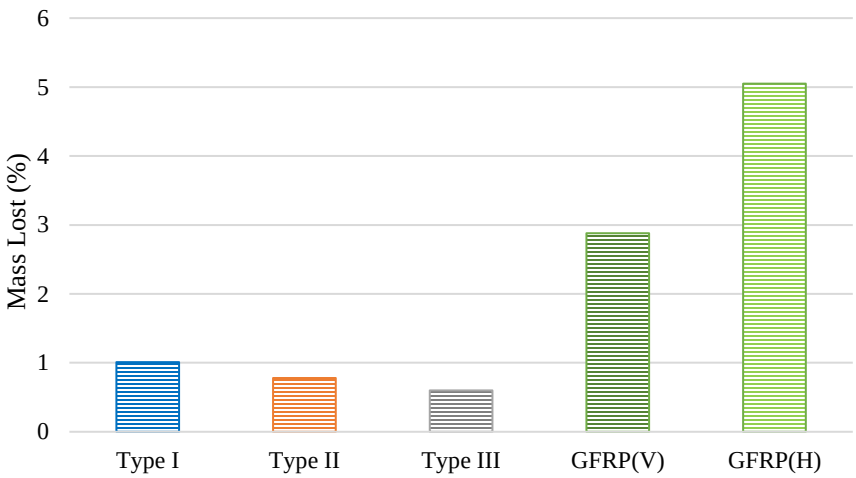

Figure 19. Mass losses of +50 ºC conditioned samples.

5. Effects of wear on tensile and compressive strength

Losses in tensile and compressive strength occur not only due to wear but also due to environmental conditions. In this research, +50°C, -50°C, and humid conditions were considered. When considering the effect of ambient conditions for concrete, it is assumed that there is no change in compressive and tensile strength at +50 °C. (BS EN 1992-1-2). At low temperatures, it has reported that strength increases as the temperature decreases (Xie, J., and Yan, J. B. 2018; Lee, G. C., Shih, T. S., and Chang, K. C. 1988). In a study conducted by Chen et al., it was observed that in the moisture level in concrete greatly influences its compressive strength, but has a much smaller impact on its tensile strength (Chen, X., Huang, W., and Zhour, J. 2012). Zhang et al. compared three concrete classes (C15, C20 and C30) with different moisture saturation. It was found that at 100% water saturation rate, there was a 27% loss of compressive strength for C15 and 21% for C20 and C30 concrete. (Zhang, G., et al. 2020). In the Böhme test, it was determined that the very slight mass and volume losses on the surfaces of the concretes did not affect the compressive and tensile strength significantly for this study.

The structure of GFRP box profiles is very different from concrete. The strength of fibrous composite materials is calculated theoretically by the following Eq 1. σ_k, σ_m , σ_l are the stresses of the composite, matrix and fiber, respectively; V_m and V_l represent the volume fraction of the matrix and fiber.

$$\sigma_k = \sigma_m x V_m + \sigma_l x V_l \qquad (1)$$

Damage to materials occurs not only due to wear but also due to the environmental conditions. It was determined by Aydin that the strength losses of the same type of GFRP material used in this study, when examined in relation to temperature, were 5.7% at +50 °C and 14.24% at -50 °C for tensile strength, and 18.24% at +50 °C and 3.4% at -50 °C for compressive strength (Aydin 2016). In the Böhme test, it was observed that the fibers in the GFRP box were not damaged as a result of wear, while the matrix material on the outer surface was worn. Assuming that a section was taken from the worn area, the tensile strength of the GFRP composite, theoretically affected by both environmental conditions and wear, is provided in Table 8

Table 8. Tensile strength of GFRP profiles exposed to different conditions and subjected to Böhme tests.

Before wear test		Non-conditioned	-50 °C conditioned	+50 °C conditioned
374.44 MPa	Vertical	370.12 MPa	318.6 MPa	350.48 MPa
	Horizontal	364.41 MPa	318.1 MPa	348.50 MPa

Since wear occurs on only one surface of the GFRP box profiles and on the outer coating of that surface and since separation of the fibers is not observed, no damage will occur in the compressive strength due to the Böhme test. However, when

the damage caused by environmental conditions are taken into account, the compressive strengths, which are 146 MPa under normal conditions, become 141.07 and 119.36 MPa for -50 ℃ and +50 ℃, respectively.

6. Monte Carlo simulation results

Monte Carlo simulation is a statistical method that uses random numbers to run an experiment multiple time. In this study, using the data obtained from experimental results, the probability of the results that can be obtained by increasing the number of experiments using the Monte Carlo method was evaluated. The probability results of the unconditioned samples and samples conditioned at +50 °C and -50 °C are given in Figures 20-22, when the number of experiments is increased to 1000. In unconditioned samples, there is more variation in GFRP profile elements. In wear tests applied on the vertical surface, the probability of mass loss is between 0.48% - 2.83% and in the horizontal direction, it is between 2.09% - 5.6%, while this range is between 0% - 2.28% for Type I, 0% - 2.63% for Type II, and 0% - 0.89% for Type III. Under hot conditions, the horizontal GFRP profiles have a mass loss ranging from 4.26% - 5.97% and the vertical profiles have a mass loss ranging from 2.25% - 3.62%, while the mass loss for Type I, II, and III are respectively in the range of 0.65% - 1.44%, 0% - 1.73%, and 0.34% - 0.89%. Under cold weather conditions, the vertical GFRP samples have a mass loss between 0% - 2.26% and the horizontal samples have a mass loss between 0% - 2.72%, with the mass losses varying between 0% - 2.71% for Type I, 0.54% - 0.83% for Type II, and 0% - 0.84% for Type III.

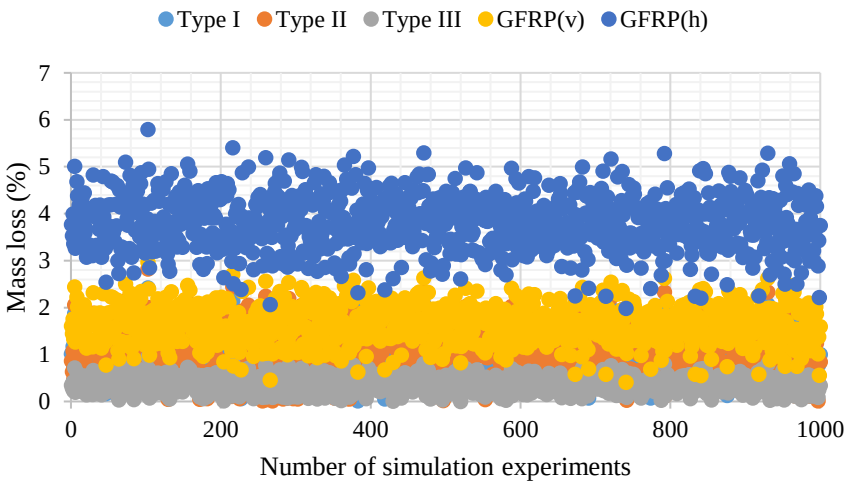

Figure 20. Monte Carlo simulation for unconditioned samples.

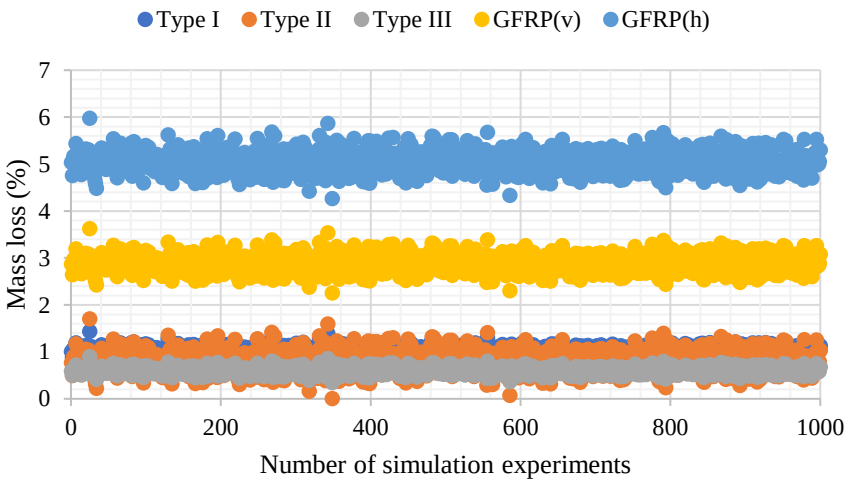

Figure 21. Monte Carlo simulation for conditioned at +50 ℃ samples.

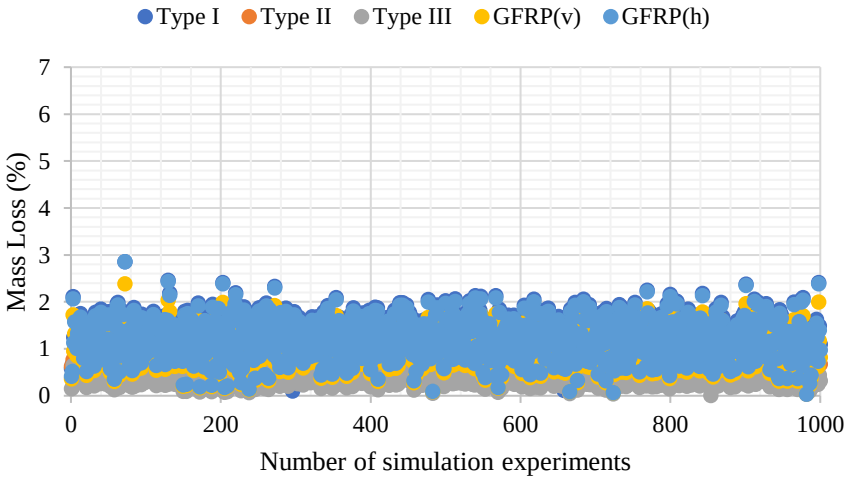

Figure 22. Monte Carlo simulation for conditioned at -50 ℃ samples.

7. Conclusion and recommendation

The results and recommendations obtained from wear tests performed on GFRP box profiles and concrete specimens under different environmental conditions are summarized below:

1. In GFRP profiles, mass losses increase by 77% in vertical tests to the fiber direction and by 33% in parallel tests at +50 °C. This rate decreases by 39% in vertical tests to the fiber direction and by 69% in parallel tests at -50 °C. Cold specimens wear approximately 3 times more in vertical tests to the fibers and 4.2 times more in parallel tests than hot specimens. Cold GFRP specimens show high performance against wear.
2. Volumetric loss rates are about 1% in both directions of the fibers. The volumetric loss rates in GFRP profiles are less than the mass loss rates.
3. Wear losses decrease as concrete strength increases. Mass losses of high-strength concretes are 22-77% less than medium-strength and low-strength concretes for 3, 7, and 28-day concretes, respectively.

4. Wear losses decrease with increasing concrete age according to concrete strength. Mass loss rates of 7-day and 3-day concretes are respectively 25-55%, 29-64%, and 125-153% higher than 28-day concretes for Type I, II, and III concretes.
5. Compared to normal conditions, humid specimens cause 50% more mass loss in high-strength concretes, hot specimens cause 67% more, and specimens kept in cold conditions cause 5% more. For Type II and Type I concretes, this situation is 17-13-0% and 7-3-4%, respectively.
6. Volumetric losses occurred in concrete specimens under all conditions and were less than 2%. Volumetric losses due to wear are like mass losses, depending on concrete age, specimen temperatures, and humidity. In humid concrete, wear increases, and specimens kept in cold weather conditions show the best wear performance.
7. Monte Carlo simulation method was used to evaluate possible probabilities by increasing the number of specimens. In unconditioned specimens, the maximum wear probabilities for mass loss are determined to be 2.83% in the vertical direction and 5.6% in the horizontal direction for GFRP profiles and 2.28%, 2.63%, and 0.89% for Type I, II, and III, respectively. In hot environments, the mass loss rate is estimated to be 5.97% and 3.62% in the vertical and horizontal GFRP profiles, respectively, and 1.44%, 1.73%, and 0.89% for Type I, II, and III concrete. Under cold conditions, maximum mass losses of 2.26% and 2.72% are expected in the vertical and horizontal GFRP profiles, respectively, and the possible maximum mass loss rates for Type I, II, and III concretes are 2.71%, 0.83%, and 0.84%, respectively.
8. GFRP profiles that lose matrix material on the surface due to wear damage the material integrity of the fibers. In addition, in applications where wear is highly likely, the design of structural elements with FRP profiles should be careful about the fiber directions.
9. Future studies may include extending the experimental conditions to extreme temperatures, chemical exposure or UV radiation and comparing the wear performance of GFRP profiles with alternative composite or hybrid materials.

Author contributions: Ferhat Aydın: Supervision, Şeymanur Arslan, Elif Toplu and Süleyman Adahi Şahin: Writer,

Funding: There is no funding for this study

Conflicts of interest: There is no conflict of interest

References

Agarwal, Gaurav, Amar Patnaik, and Rajesh Kumar Sharma. (2014). "Comparative Investigations on Three-Body Abrasive Wear Behavior of Long and Short Glass Fiber-Reinforced Epoxy Composites." http://dx.doi.org/10.1080/09243046.2013.868661 23(4): 293–317.

AlAjarmeh, O., Manalo, A., Benmokrane, B., Schubel, P., Zeng, X., Ahmad, A., ... and Sorbello, C. D. (2022). "Compression behavior of GFRP bars under elevated In-Service temperatures". Construction and Building Materials, 314, 125675..

Aliasghar-Mamaghani, Mojtaba, and Alireza Khaloo. (2018). "Seismic Behavior of Concrete Moment Frame Reinforced with GFRP Bars." https://doi.org/10.1016/j.compositesb.2018.10.082

Arslan, Ş., and Aydın, F. (2023)." Experimental Investigation of the Effects of Insulation Materials and Concrete Strength on Temperature Transitions in FRP Reinforced Structural Elements Under High Temperature". Gazi University Journal of Science Part C: Design and Technology, 11(1), 222-235. https://doi.org/10.29109/gujsc.1167810

Ashrafi, H., Bazli, M., Jafari, A., and Ozbakkaloglu, T. (2020). "Tensile properties of GFRP laminates after exposure to elevated temperatures: Effect of fiber configuration, sample thickness, and time of exposure." Composite Structures, 238, 111971.

Atiş, Cengiz Duran. (2002). "High Volume Fly Ash Abrasion Resistant Concrete." Journal of Materials in Civil Engineering 14(3): 274–77.

Aydin, Ferhat. (2016). "Effects of Various Temperatures on the Mechanical Strength of GFRP Box Profiles." Construction and Building Materials 127: 843–49. http://dx.doi.org/10.1016/j.conbuildmat.2016.09.130.

Aydın, F., Akyürek, M., Arslan, Ş., and Yılmaz, K. (2023). "Effects of concrete cover thickness and concrete strength on temperature transfer in high temperature exposed FRP reinforced concrete". Revista de la construcción, 22(1), 242-258. https://doi.org/10.7764/RDLC.22.1.242

Aydın, F., and Arslan, Ş. (2021). "Investigation of the durability performance of FRP bars in different environmental conditions." Advances in concrete construction, 12(4), 295-302. DOI: https://doi.org/10.12989/acc.2021.12.4.295

Aydın, F., Sarıbıyık, A., Sarıbıyık M., Ipek M. (2018). "Experimental Study of Flexural Performance of Reinforced Concrete Beams and Hybrid Beams", ACTA PHYSICA POLONICA A, Vol. 134, No.1. DOI: 10.12693/APhysPolA.134.244

Aydın F. ve Sarıbıyık M., (2010). "Compressive and Flexural Behavior of Hybrid Use of GFRP Profile with Concrete." ISSD 2010, International Symposium on Sustainable Development, Sarajevo, Bosnia and Herzegovina, 8-11 June 2010.

Bakis, C. E. et al.(2003). "Fiber-Reinforced Polymer Composites for Construction - State-of-the-Art Review." Perspectives in Civil Engineering: Commemorating the 150th Anniversary of the American Society of Civil Engineers: 369–83.

Bazli, M., and Abolfazli, M. (2020). "Mechanical properties of fibre reinforced polymers under elevated temperatures: An overview." Polymers, 12(11), 2600. https://doi.org/10.3390/polym12112600

BS EN 1992-1-2:2004 (2005) Eurocode 2: Design of Concrete Structures. General Rules. Structural Fire Design, European Committee for Standardization, Brussels,

CAN/CSA-S806-02. (2009). Design and Construction of Building Components with Fibre-Reinforced Polymers.

Chand, N., A. Naik, and S. Neogi. (2000). "Three-Body Abrasive Wear of Short Glass Fibre Polyester Composite." Wear 242(1–2): 38–46.

Chandru, B. G., and Shivashankar, G. S. (2012). "Preparation and Evaluation of Mechanical and Wear Properties of Hybrid FRP Composites." Int. J. Mech. Eng. and Rob. Res.

Chen, X., Huang, W., and Zhour, J. (2012). "Effect of moisture content on compressive and split tensile strength of concrete." Indian Journal of Engineering and Materials Sciences Vol. 19, December 2012, pp. 427-435

Choi, Ki Sun, Dongkeun Lee, Young Chan You, and Sang Whan Han. (2022). "Long-Term Performance of 15-Year-Old Full-Scale RC Beams Strengthened with EB FRP Composites." Composite Structures 299: 116055.

Christian, S. J., and S. L. Billington. (2011). "Mechanical Response of PHB- and Cellulose Acetate Natural Fiber-Reinforced Composites for Construction Applications." Composites Part B: Engineering 42(7): 1920–28.

Das, Diptikanta et al. (2019). "Mechanical Properties and Abrasion Behaviour of Glass Fiber Reinforced Polymer Composites – A Case Study." Materials Today: Proceedings 19: 506–11.

Dweib, M. A. et al. (2004). "All Natural Composite Sandwich Beams for Structural Applications." Composite Structures 63(2): 147–57.

Harsha, A. P., and Sanjeev Kumar Jha. (2008). "Erosive Wear Studies of Epoxy-Based Composites at Normal Incidence." Wear 265(7–8): 1129–35.

Hawileh, R. A., Abu-Obeidah, A., Abdalla, J. A., and Al-Tamimi, A. (2015). "Temperature effect on the mechanical properties of carbon, glass and carbon–glass FRP laminates." Construction and building materials, 75, 342-348. https://doi.org/10.1016/j.conbuildmat.2014.11.020

He, Zhen, Xiaorun Chen, and Xinhua Cai. (2019). "Influence and Mechanism of Micro/Nano-Mineral Admixtures on the Abrasion Resistance of Concrete." Construction and Building Materials 197: 91–98.

Hollaway, L. C. (2010). "A Review of the Present and Future Utilisation of FRP Composites in the Civil Infrastructure with Reference to Their Important In-Service Properties." Construction and Building Materials 24(12): 2419–45.

Jarrah, M., Najafabadi, E. P., Khaneghahi, M. H., and Oskouei, A. V. (2018). "The effect of elevated temperatures on the tensile performance of GFRP and CFRP sheets." Construction and Building Materials, 190, 38-52. https://doi.org/10.1016/j.conbuildmat.2018.09.086

Jiang, Xu, Henk Kolstein, and Frans S.K. Bijlaard. (2013). "Moisture Diffusion in Glass–Fiber-Reinforced Polymer Composite Bridge under Hot/Wet Environment." Composites Part B: Engineering 45(1): 407–16.

Jumahat, A., S. Kasolang, and M.T. Bahari. (2015). "Wear Properties of Nanosilica Filled Epoxy Polymers and FRP Composites." Jurnal Tribologi 6: 24–36.

Keller, Thomas. (2001). "Recent All-Composite and Hybrid Fibre-Reinforced Polymer Bridges and Buildings." Progress in Structural Engineering and Materials 3(2): 132–40. https://onlinelibrary.wiley.com/doi/full/10.1002/pse.66

Khaneghahi, M. H., Najafabadi, E. P., Bazli, M., Oskouei, A. V., and Zhao, X. L. (2020). "The effect of elevated temperatures on the compressive section capacity of pultruded GFRP profiles." Construction and Building Materials, 249, 118725. https://doi.org/10.1016/j.conbuildmat.2020.118725

Kiliç, A. et al. (2008). "The Influence of Aggregate Type on the Strength and Abrasion Resistance of High Strength Concrete." Cement and Concrete Composites 30(4): 290–96.

Kumarasamy, S., Abidin, M. S. Z., Bakar, M. A., Nazida, M. S., Mustafa, Z., and Anjang, A. (2018, May). "Effects of high and low temperature on the tensile strength of glass fiber reinforced polymer composites." In IOP conference series: materials science and engineering (Vol. 370, No. 1, p. 012021). IOP Publishing.

Lasri, L., M. Nouari, and M. El Mansori. (2011). "Wear Resistance and Induced Cutting Damage of Aeronautical FRP Components Obtained by Machining." Wear 271(9–10): 2542–48.

Lee, G. C., Shih, T. S., and Chang, K. C. (1988). "Mechanical properties of concrete at low temperature." Journal of cold regions engineering, 2(1), 13-24.

Lee, Sung Woo, Kee Jeung Hong, and Sinzeon Park. (2018). "Current and Future Applications of Glass-Fibre-Reinforced Polymer Decks in Korea." https://doi.org/10.2749/101686610793557672 20(4): 405–8. https://www.tandfonline.com/doi/abs/10.2749/101686610793557672 (October 14, 2022).

Liu, Yu-Wen, Shi-Wei Cho, and Tsao-Hua Hsu. (2012). "IMPACT ABRASION OF HYDRAULIC STRUCTURES CONCRETE." Journal of Marine Science and Technology 20(3): 253–58. https://jmstt.ntou.edu.tw/journal/vol20/iss3/2 (October 14, 2022).

Liu, Yu Wen.(2007). "Improving the Abrasion Resistance of Hydraulic-Concrete Containing Surface Crack by Adding Silica Fume." Construction and Building Materials 21(5): 972–77.

Mansouri, Iman, Farzaneh Sadat Shahheidari, Seyyed Mohammad Ali Hashemi, and Alireza Farzampour. (2020). "Investigation of Steel Fiber Effects on Concrete Abrasion Resistance." Advances in concrete construction 9(4): 367–74.

Najafabadi, Esmaeil Pournamazian, Milad Bazli, Hamed Ashrafi, and Asghar Vatani Oskouei. (2018). "Effect of Applied Stress and Bar Characteristics on the Short-Term Creep Behavior of FRP Bars." https://doi.org/10.1016/j.conbuildmat.2018.03.

Nochaiya, Thanongsak, Tawat Suriwong, and Phongthorn Julphunthong. (2022). "Acidic Corrosion-Abrasion Resistance of Concrete Containing Fly Ash and Silica Fume for Use as Concrete Floors in Pig Farm." Case Studies in Construction Materials 16: e01010.

Nystrom, Halvard E., Steve E. Watkins, Antonio Nanni, and Susan Murray.(2003). "Financial Viability of Fiber-Reinforced Polymer (FRP) Bridges." Journal of Management in Engineering 19(1): 2–8. https://ascelibrary.org/doi/abs/10.1061/%28ASCE%290742-597X%282003%2919%3A1%282%29 (October 14, 2022).

Omoding, Nicholas, Lee S. Cunningham, and Gregory F. Lane-Serff. (2021a). "Effect of Using Recycled Waste Glass Coarse Aggregates on the Hydrodynamic Abrasion Resistance of Concrete." Construction and Building Materials 268: 121177.

Omoding, Nicholas, Lee S. Cunningham, and Gregory F. Lane-Serff. (2021b). "Influence of Coarse Aggregate Parameters and Mechanical Properties on the Abrasion Resistance of Concrete in Hydraulic Structures." Journal of Materials in Civil Engineering 33(9): 04021244.

Özkal, F. M., Polat, M., Yağan, M., and Öztürk, M. O. (2018). "Mechanical properties and bond strength degradation of GFRP and steel rebars at elevated temperatures." Construction and Building Materials, 184, 45-57. https://doi.org/10.1016/j.conbuildmat.2018.06.203

Pihtili, Hasim.(2009). "An Experimental Investigation of Wear of Glass Fibre–Epoxy Resin and Glass Fibre–Polyester Resin Composite Materials." European Polymer Journal 45(1): 149–54.

Ramesh Kumar, G. B., and U. K. Sharma. (2014). "Abrasion Resistance of Concrete Containing Marginal Aggregates." Construction and Building Materials 66: 712–22.

Sadegzadeh, M., C. L. Page, and R. J. Kettle. (1987). "Surface Microstructure and Abrasion Resistance of Concrete." Cement and Concrete Research 17(4): 581–90.

Sarıbıyık, M, A. Cumhur, F. Aydın, and A Sarıbıyık. (2007). "Pultruzyon Metodu İle Üretilen Cam Fiber Takviyeli Plastik Profillerin Sera Modellemesinde Kullanılması." In International Symposium on Advances in Earthquake and Structural Engineering, Antalya, Türkiye, 674–82.

Shahrbijari, K. B., Barros, J. A., and Valente, I. B. (2024). "Experimental study on the structural performance of concrete beams reinforced with prestressed GFRP and steel bars." Construction and Building Materials, 438, 137031.

Sharbaf, Mohammadreza, Meysam Najimi, and Nader Ghafoori. (2022). "A Comparative Study of Natural Pozzolan and Fly Ash: Investigation on Abrasion Resistance and Transport Properties of Self-Consolidating Concrete." Construction and Building Materials 346: 128330.

Silva, Cristina V., Janete E. Zorzi, Robinson C.D. Cruz, and Denise C.C. Dal Molin. (2019). "Experimental Evidence That Micro and Macrostructural Surface Properties Markedly Influence on Abrasion Resistance of Concretes." Wear 422–423: 191–200.

Singh, Prathu et al. (2022). "Characterization of Wear of FRP Composites: A Review." Materials Today: Proceedings 64: 1357–61.

Srivastava, V. K. (2006). "Effects of Wheat Starch on Erosive Wear of E-Glass Fibre Reinforced Epoxy Resin Composite Materials." Materials Science and Engineering: A 435–436: 282–87.

Srivastava, V. K., and S. Wahne. (2007). "Wear and Friction Behaviour of Soft Particles Filled Random Direction Short GFRP Composites." Materials Science and Engineering: A 458(1–2): 25–33.

Suresha, B. et al. (2010). "Influence of Graphite Filler on Two-Body Abrasive Wear Behaviour of Carbon Fabric Reinforced Epoxy Composites." Materials and Design 31(4): 1833–41.

Suresha, B., G. Chandramohan, Siddaramaiah, and T. Jayaraju. (2008). "Three-Body Abrasive Wear Behavior of E-Glass Fabric Reinforced/Graphite-Filled Epoxy Composites." Polymer Composites 29(6): 631–37. https://onlinelibrary.wiley.com/doi/full/10.1002/pc.20447 (October 15, 2022).

Suresha, B., and Kunigal N.Shiva Kumar. (2009). "Investigations on Mechanical and Two-Body Abrasive Wear Behaviour of Glass/Carbon Fabric Reinforced Vinyl Ester Composites." Materials and Design 30(6): 2056–60.

Teng, J. G., J. F. Chen, S. T. Smith, and L. Lam. (2003). "Behaviour and Strength of FRP-Strengthened RC Structures: A State-of-the-Art Review." Proceedings of the Institution of Civil Engineers: Structures and Buildings 156(1): 51–62.

Teng, J G et al. (2002). "FRP-Strengthened RC Structures." In Wiley, London, UK.

Tewari, U. S., A. P. Harsha, A. M. Häger, and K. Friedrich. (2003). "Solid Particle Erosion of Carbon Fibre– and Glass Fibre–Epoxy Composites." Composites Science and Technology 63(3–4): 549–57.

TS 2824. (2005). EN 1338 Zemin Döşemesi İçin Beton Kaplama Blokları-Gerekli Şartlar Ve Deney Metotları. Ankara, Türkiye.

Xie, J., and Yan, J. B. (2018). "Experimental studies and analysis on compressive strength of normal-weight concrete at low temperatures." Structural Concrete, 19(4), 1235-1244.

Wang, Lei et al. (2021). "Pore Structural And Fractal Analysis Of The Influence Of Fly Ash And Silica Fume On The Mechanical Property And Abrasion Resistance Of Concrete." https://doi.org/10.1142/S0218348X2140003X 29(2): 2140003.

Zarrabi, Navid, Mohammad Navid Moghim, and Mohammad Reza Eftekhar. (2021). "Effect of Hydraulic Parameters on Abrasion Erosion of Fiber Reinforced Concrete in Hydraulic Structures." Construction and Building Materials 267: 120966.

Zhang, G., Li, C., Wei, H., Wang, M., Yang, Z., and Gu, Y. (2020). "Influence of humidity on the elastic modulus and axis compressive strength of concrete in a water environment." Materials, 13(24), 5696.